Research Article

Versatile synthesis of activated carbon from coconut shells: a method for cyanide adsorption in artisanal and small-scale gold mining wastewater

Achmad Gus Fahmi[1], Zaenal Abidin[2*], Cecep Kusmana[3], Erliza Noor[4]

[1] Graduate School of Natural Resources and Environmental Management Science, IPB University, Bogor, 16127, Indonesia
[2] Department of Chemistry, IPB University, Bogor, 16680 Indonesia
[3] Department of Silviculture, IPB University, Bogor, 16680 Indonesia
[4] Department of Agro-Industrial Engineering, IPB University, Bogor, 16680 Indonesia

*corresponding author: abidinzed@apps.ipb.ac.id

Abstract

Over the next years, Indonesia's traditional gold mining technique (that employs mercury amalgamation) will be gradually replaced by cyanidation as a result of a Presidential Decree that has been recently issued. The cyanide-containing waste resulting from the processing tanks of this new method will be generally sedimented and flow directly into the surrounding small rivers. This study aimed to reduce the impact of cyanide contamination on the environment by using the simple activated carbon that can be produced by artisanal and small-scale gold mining (ASGM). Water samples were taken from artificial wastewater as part of three replications. The highest recorded removal of cyanide from sewage was 98.43%, with an equilibrium reached at a fixed adsorbent dosage of 0.05 g over a contact time of 24 hours. Cyanide adsorption was also found to be pH-dependent, with the highest cyanide adsorption occurring at a pH of 8. The adsorption capacity for cyanide was estimated at 12.51 mg g^{-1} of the adsorbent, and it was considered to function based on a Langmuir isotherm model. The findings of this study confirm that the utilized glass wool in the assessed method can increase the yield of activated carbon, thereby offering a low-cost and effective adsorbent that can be used in order to remove cyanide from ASGM wastewater.

Introduction

Gold is one of the most expensive metals, yet it is usually mined under hazardous conditions for the artisanal and small-scale gold miners' health (Knoblauch et al., 2020; Gafur et al., 2022; Taux et al., 2022). Liquid mercury has been used in simple gold extraction by traditional gold miners, but it is dangerous and exposes them to a high level of this toxic heavy metal (Prasetia et al., 2022). In fact, traditional gold miners have employed liquid mercury in various places in Indonesia since the colonial era (Soemarwoto et al., 2010). A previous study has shown that the conventional changes in land use and landscapes, the instability of the ground, the erosion of sand water, and the pollution of the water and the soil are common problems associated with gold mining activities (Muslihudin et al., 2018; Basir-Cyio et al., 2020; Githiria et al., 2020). Moreover, the latter is known to exert both positive and negative socio-economic impacts (Anggraini et al., 2019).

Recently in Indonesia, liquid mercury has been banned as a gold extraction technique. Presidential Decree #21 of 2019 concerning the national action plan for mercury elimination enforced the gradual replacement of the technique allowing for the

extraction of gold through mercury amalgamation by cyanidation (Verbrugge et al., 2021). As a result of this requirement, cyanides will be used in order to extract gold from the ore. However, the residual material will be rich in cyanide ions and will eventually be released into the environment without treatment or control. Consequently, this new gold mining technique will result in cyanide pollution around the mining settings.

The cyanide concentration used in artisanal small-scale gold mining (ASGM) is usually about 1:12 parts cyanide in the total rock. In Sekotong, West Nusa Tenggara, cyanide levels at the soil surface range from 63.93 to 104.08 mg kg^{-1}, and they are also observed in plants at levels ranging from 18.41 to 52.85 mg kg^{-1} (Suhadi et al., 2021). However, these levels may vary from place to place, depending on the rock type and the cyanide concentration used. Studies on cyanide removal are mainly focused on industrial wastewater (Esparza et al., 2019); however, the study of cyanide removal in gold leaching tailings in ASGM, which contain both wastewater and tailings, is still limited. In addition, the presence of cyanide in the water can cause death (Jaszczak et al., 2017). Therefore, cyanide must be reduced by using relatively simple materials that can be easily obtained by traditional miners, and activated carbon could serve as such.

Activated carbon has already been used as an absorber of pollutants for organic matter in the environment, including cyanide (Jiao et al., 2016). High-molecular-weight compounds are usually absorbed by the activated carbon mesoporous, while low-molecular-weight compounds can be absorbed by the micropore (Li et al., 2012). The surface area, the pore sizes, and the functional groups found in activated carbon determine its adsorption characteristics. However, the most decisive aspects of its effectiveness are the raw materials used for it and its activation (Bansal and Goyal, 2005). Naturally, carbon will be formed as part of the biomass carbonization process that will be spread on the soil and sediment. The lignocellulose obtained from biomass will be converted into black carbon (Xiao et al., 2018). While, synthetically, carbon is made by burning biomass at 280°C, it can be burned out if carbonization occurs above 700 °C (Han et al., 2016). In fact, the higher the combustion temperature used, the more carbon is lost due to oxidation. Therefore, the activating of carbon at temperatures above 700 °C is carried out under conditions involving the absence of oxygen (pyrolysis). Pyrolysis is usually carried out in airtight chambers or with the continuous addition of inert gases such as nitrogen (Sun et al., 2017) and water vapors (Bhandari and Gogate, 2017).

The pyrolytic process can be done by using adequate tools so that only certain people can use it. Modifications of the pyrolytic process can allow for wider use by the community. Pyrolysis using an aluminum foil cover has been achieved and can fix the fragility of the activated carbon that is produced from bamboo (Park et al., 2009). However, the aluminum foil will be damaged at high temperatures, and as a result, its utilization is limited to high temperatures. The use of other materials that can have a similar function as heat and air insulators needs to be further studied. Glass wool is a well-known insulating material (Jeon et al., 2017), and it has the potential to act as a cover material under the high-temperature conditions required for pyrolysis. In this study, we aimed to identify the effect of glass wool on the pyrolytic process of the activated carbon formed and to examine the characteristics and the suitability of the latter in absorbing cyanide ions.

Materials and Methods

Coconut shell waste was obtained from coconut sellers at the Dramaga Market, Bogor. Glass wool brand R9 and all the chemicals used were obtained from Sigma-Aldrich, while the commercially available activated carbon used as a control was purchased from the chemical store in Bogor City, West of Java.

Preparation and synthesis of activated carbon

Coconut shells were separated from the coir or the coconut fiber and were then air-dried under direct sunlight for approximately 3 days. Subsequently, the coconut shells were smoothed by using a Thomas Model 4 Wiley ® Mill machine (Thomas Scientific, USA) with a power of 5,000-6,000 rpm until they reached 100 mesh in size. The synthesis of activated carbon was undertaken based on a modified method by Fahmi et al. (2019) that involved the mashed coconut shell being placed into a cup that was coated with glass wool (ACG) and aluminium foil (ACA) on the top and all around. The cup was then heated at a temperature of 750 °C with a 47900 Thermoline furnace (Barnstead International, USA) for 3 hours, and the yield obtained was calculated using the following equation (Efeovbokhan et al., 2019):

$$\%\text{Yield (w/w)} = \frac{\text{mass (g) of activated carbon}}{\text{mass (g) of biomass}} \times 100 \dots (1)$$

Measurement of the physicochemical properties of activated carbon

The activated carbon-specific surface area was determined by using semi-quantitative measurements (Okeola et al., 2012; Fahmi et al., 2021). The characterization of the activated carbon was carried out to determine its physicochemical properties. Physicochemical properties of the activated carbon (such as pH, ash content, and moisture content) were determined by using standard methods. The pH of the activated carbon was determined by following the ASTM D3838-80 protocol, where 1 g of the activated carbon was introduced into 100 mL of distilled water in a 250 mL beaker glass, was stirred continuously for

10 min, and was then filtered, and the pH of the filtrate solution was analyzed by using a pH meter. The activated carbon ash content was determined by using the ASTM D2866-96 protocol, and the moisture content was determined by using the oven-drying method described in the ASTM D2867-09 protocol. The cation exchange capacity (CEC) of activated carbon was determined according to Munera-Echeverri et al. (2018). Functional groups were assessed by using a Perkin-Elmer Spectrum One Fourier Transform Infrared.

Adsorption experiment

The investigation of cyanide adsorption onto the activated carbon was conducted by using a batch experiment. The adsorption technique was conducted in a batch system, and a centrifuge tube containing 5 mL of artificial wastewater was used for it. The batch units were shaken every 30 min and assessed by using a Universal pH paper. The effect of the different experimental parameters was assessed by varying the pH (6, 7, 8, 9, 10, 11, and 12) that was adjusted by using a 1-M NaOH solution, the contact time (0.5, 1, 3, 6, 12, 18, and 24 h), and the adsorbent dosage (0.01, 0.05, 0.10, 0.50, and 1.00 g). The isotherm adsorption of cyanide on the sample was carried out by adding 0.01 g of each sample into 1 ml of cyanide ion solution with various concentrations (1-500 ppm) at room temperature and shaken for 24 hours. The cyanide concentration in the supernatant was measured after being separated from the adsorbent.

The measurement of cyanide in the wastewater and in the stock solution was conducted according to the modified method of Surleva et al. (2013) and Tabian et al. (2022) by using a UV-Vis spectrophotometer Jenway 7300 (Cole-Parmer, UK). Sample and wastewater were allowed to react with 4 mL of 2% ninhydrin in a base solution (4 mL of 10% Na_2CO_3) for 15 min (until the reaction was complete). After the reaction equilibrium time (15-30 min) was reached, the sample was immediately proceeded to measure cyanide to reduce the chances of any measurement errors. To calculate the adsorption capacity (q_e) and the percentage removal efficiency (%E), the following equations were used (Eke-emezie and Etuk, 2019):

$$q_e = \frac{(C_o\text{-}C)}{m} \text{ x } V ....(2)$$

$$f\%E = \frac{C_o\text{-}C}{C_o} x\ 100 ....(3)$$

where q_e stands for the adsorption capacity (mg g^{-1} adsorbent), E stands for the removal efficiency (measured as $E\%$), V is the volume of the solution (mL), C_o is the initial cyanide concentration (mg L^{-1}), C represents the residual cyanide concentration (mg L^{-1}), and m stands for the weight of the adsorbent (g). Langmuir and Freundlich's isotherms were used to understand cyanide adsorption on the adsorbent surface, and the calculations referred to Bhandari and Gogate (2017).

Results and Discussion

Physicochemical properties of the activated carbon

The yield resulting from the activated carbon after carbonization at a temperature of 750 °C without treatment obtained the lowest percentage value, namely, 8.74%. The increasing importance of the yield percentage occurs when materials such as aluminium foil and glass wool are used as a cover or are placed around the cup. The use of these materials is that they can prevent oxygen from reacting with carbon so that the latter can increase the yield. By using aluminum foil and glass wool as a cup cover, one can produce a lower activated carbon yield. The difference in these conditions is very significant, as shown in Figure 1. The highest result was obtained by using glass wool around the cup, which is equal to 42.88%; on the other hand, the use of aluminum foil returned a 20.02% yield. The temperature and time of carbonization greatly influence the yield obtained. The higher the temperature and the longer the carbonization time, the lower the percentage of yield produced (Park, 2018).

Aluminum foil is used for food packaging, cosmetics, and chemical products and for industrial thermal, cable, and electronic insulation applications. In addition, aluminum foil can reduce air penetration, a property that makes it particularly suitable for use in the carbonization process (Kubik and Zeman, 2014). In fact, the use of aluminum foil as a coating in the carbonization process is known to reduce the cracking of the bamboo carbon produced (Park et al., 2009). However, at temperatures above 700 °C, the aluminum foil can contaminate the obtained carbon as it begins to decompose and collapse at this temperature.

By modifying the carbonization method with the use of glass wool, the latter–aside from acting as a "blanket"–can also reduce the ash formed (Figure 1). The ash created during the production of activated carbon can reduce its quality. Air is one of the worst thermal conductors, while glass wool is an insulating material that can isolate heat well (Jeon et al., 2017). The heat isolated causes a heat distribution in the cup, allowing for the carbonization process to be evenly distributed and reducing ignition. The physical properties of the activated carbon are presented in Table 1. The results show that the specific surface area of the ACG is high at 751 m^2 g^{-1}. The increased surface area indicates a high adsorptive capacity for an adsorbent (Evbuomwan et al., 2013). The ash content is a property that is very important in determining the quality of an adsorbent, with a suitable adsorbent having as low of an ash content as possible <10% (De Gisi et al., 2016). This is due to the fact that the high ash content reduces the adsorptive capacity of the adsorbent and lowers the specific surface area. The ash content of ACG was 5.10%, which is relatively low.
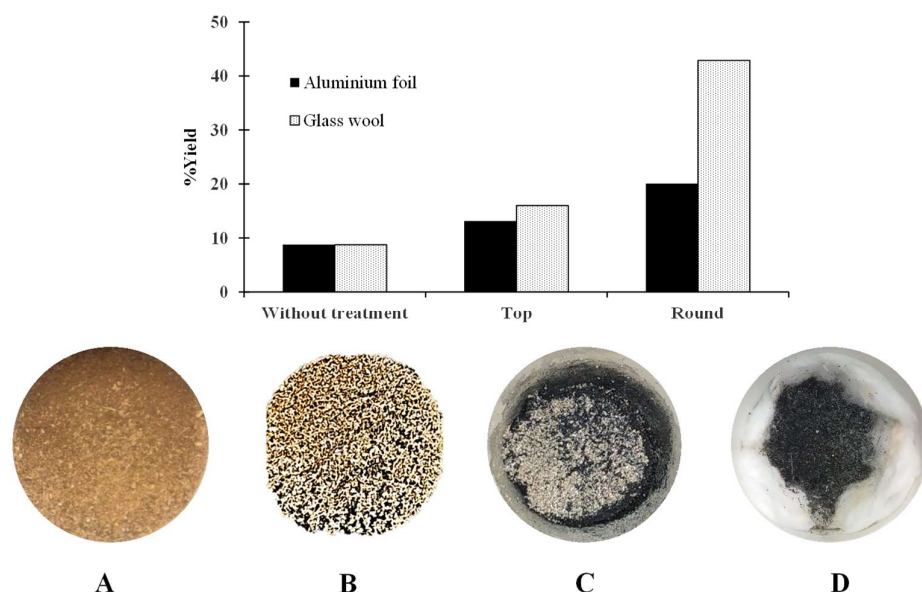
Figure 1. Yield percentages after various treatments: biomass surface (A), the surface of biomass without treatment after carbonization process (B), the ACA surface after aluminium foil treatment (C), and the ACG surface after glass wool treatment (D).

The pH affects the rate of adsorption of an adsorbent. The pH of the ACG was found to be close to neutral and generally within the acceptable range of a pH of 6–8 which is suitable for general applications in the treatment of wastewater (Ashtaputrey and Ashtaputrey, 2016). The moisture content of the ACG was low (at 4.94%), which indicates that the ACG was handled correctly; the latter is justified by the fact that the moisture content dilutes the adsorbent, thereby requiring the use of additional adsorbent weight during the treatment process to maintain the same adsorptive capacity (Mariana et al., 2017).

In this study, the value of cation exchange capacity (CEC) ranged from 470 to 616.05 $cmol_{(+)}$ kg^{-1} (Table 1). The test was carried out in a neutral solution condition (pH=7). The test results showed that ACG had the highest CEC value (616.05 $cmol_{(+)}$ kg^{-1}). This strengthens the surface properties of ACG in tests using infrared spectra and CEC that the functional groups on the surface are different from the functional groups present in the initial biomass. Increasing the density of surface functional groups can also increase the exchangeable cation of activated carbon at a certain pH (Sivakumar et al., 2012). The ACC has no functional groups on the surface (Figure 2). The presence of a pore structure and residual combustion ash can give an error measuring of CEC of activated carbon (Danish et al., 2011).

Table 1. Physicochemical properties of the activated carbon.

Parameter	ACG	ACC	ACA	Biomass
Specific surface area ($m^2 g^{-1}$)	751 ± 10	783 ± 10	712 ± 10	407 ± 10
Ash content (%)	5.10 ± 1.0	3.10 ± 1.0	5.08 ± 1.0	5.15 ± 1.0
pH	6.80 ± 0.2	6.98 ± 0.2	6.78 ± 0.2	-
Moisture content (%)	4.94 ± 1.0	3.94 ± 1.0	3.41 ± 1.0	14.94 ± 1.0
Cation exchange capacity (CEC) in pH 7 ($cmol_{(+)} kg^{-1}$)	616.05	470.00	593.01	572.77

The characteristics of the activated carbon produced by the modified carbonization method employing glass wool are different from those of the activated carbon by using aluminum foil. The identification of functional groups can be seen in the infrared spectrum produced (Figure 2). The functional groups detected through molecular vibrations in carbon after applying the glass wool method (ACG) are the hydroxyl (O–H) group (at wavenumbers of 3,000-3,400 cm^{-1}) and carboxyl (C=O) group (at wavenumbers of 1,600-1,800 cm^{-1}) (Yakout and El-Deen, 2016). These functional groups have similarities with the initial biomass of the raw material (coconut shells) used for making activated carbon. Our findings suggest that the performed carbonization method maintains these functional groups. The presence of these functional groups can affect the ability of adsorption to cations and anions.
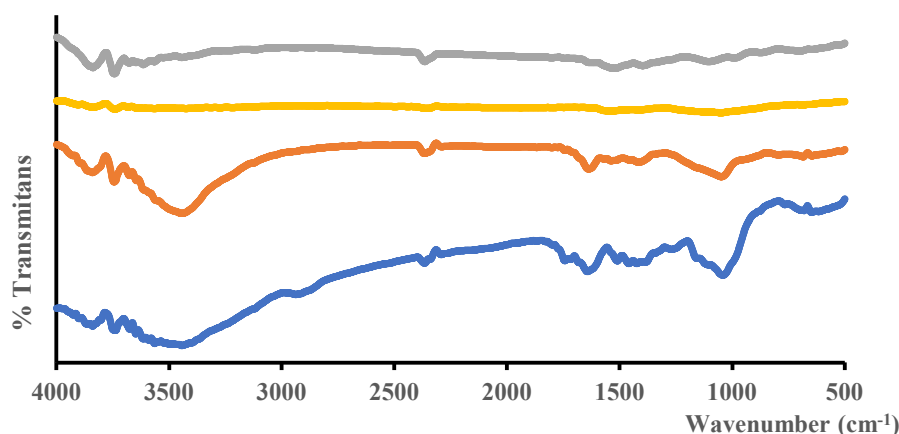
Figure 2. Infrared (IR) spectrum of biomass (blue line), ACG (red line), ACA (orange line), and ACC (grey line).

In addition, the hydroxyl and carboxyl functional groups can affect the characteristics of the carbon surface produced; in fact, the more decreased the hydroxyl and the carboxyl functional groups appear to be, the more hydrophobic the activated carbon characteristics are made (Jiao et al., 2016). Meanwhile, in ACA and ACC the hydroxyl and carboxyl group spectrum disappear.

Cyanide adsorption into activated carbon

The ACG was tested for cyanide ions' adsorption with influenced variables such as pH, adsorbent dosage and contact time (Figure 3). The influence of the pH solution is known to affect the species (variable charge) of cyanide and lead on the adsorbent surface (Johnson, 2015; Knoblauch et al., 2020). The amount of cyanide removed from wastewater increases until a pH of 9 and decrease with the increasing pH. Due to their relative abundances, the cyanide species depend on the pH (in fact, CN^- is the dominant cyanide form at high pH, conditions) and on the pKa changes as a result of temperature variations. CN^- and HCN are likewise affected by the ionic strength; however, the influence of the latter is minor (Bernal et al., 2017). The maximum cyanide that can be adsorbed from wastewater is at a pH of 8 with percentage adsorption of 86.00% and then decreased to around 79.67% at a more basic pH. This trend is in line with the state of cyanide species (CN^-) where the active site of ACG is negatively charged, thereby resulting in a reduction of its adsorption capacity. Comparison with other studies has also shown a decrease in terms of the adsorption capacity (Bernal et al., 2017; Al-Ghouti et al., 2020). On the other hand, this condition could be advantageous if the surface-active side of the adsorbent was positively charged, on the condition that the adsorption isotherm followed the Langmuir adsorption isotherm (Table 2).

The influence of the adsorbent dosage on cyanide adsorption demonstrated a steady rise in the percent removal of cyanide from 81.32% at an

adsorbent dosage of 0.05 g to 91.54% at an adsorbent dosage of 1.00 g. The active site on the surface area is known to overlap at a higher dosage and block the adsorbate interaction (Eletta et al., 2016). Hence, only 0.05 g of the adsorbent dosage was used in the conducted adsorption experiment, as larger doses might not prove cost-effective.

The investigation of the effect of the contact time on the adsorption process was found to be particularly slow between the first hour of the contact and up until the equilibrium was reached (24 hours). The percentage of cyanide removal increased from 64.32% to 98.34% within these 24 hours. After the equilibrium was reached, the contact time did not exert any significant change on the adsorption performance. The saturation of the active binding site and the equilibrium time are believed to be the main reasons for this phenomenon. This situation usually occurs during the adsorption process when applying the batch method; in that case, obtaining the contact time data is essential. According to Istratie et al. (2019), the contact time can significantly affect the operational costs when developing adsorbents for large-scale applications.

The maximum adsorption capacity of ACA and ACG was 3.687 and 6.993 mg g^{-1}, respectively (Figure 4). This value is lower when compared to ACC (9.276 mg g^{-1}). The adsorption capacity of biomass (0.595 mg g^{-1}) is the lowest compared to the others. This indicates that the presence of a charge on the surface of activated carbon can reduce the adsorption ability of activated carbon. The adsorption of cyanide ions is influenced by the temperature, the pH, and the ionic strength. When compared to other studies, the adsorption of cyanide ions at a pH of 10 and an increase in the adsorption temperature are expected to increase the adsorption capacity of the activated carbon (Knoblauch et al., 2020).

The isotherm model is shown in Table 1 and closely conforms to the Langmuir model for ACC, ACG, ACA, and biomass behavior until reaching an equilibrium concentration. According to Hou et al.

(2020), gold leaching wastewater will leach at a 35% rate, with a final pH of 10.78. In China, tailings have a total carbon content of 2.47-6.67%, with an organic carbon concentration of 1.47-4.29%. The temperature of the solution was maintained at 23.2 °C. The average cyanide concentration of the ASGM wastewater is 11.78 mg L^{-1}, while the cyanide value of tolerance in the surface water is 0.2 mg L^{-1} (US EPA, 2020).
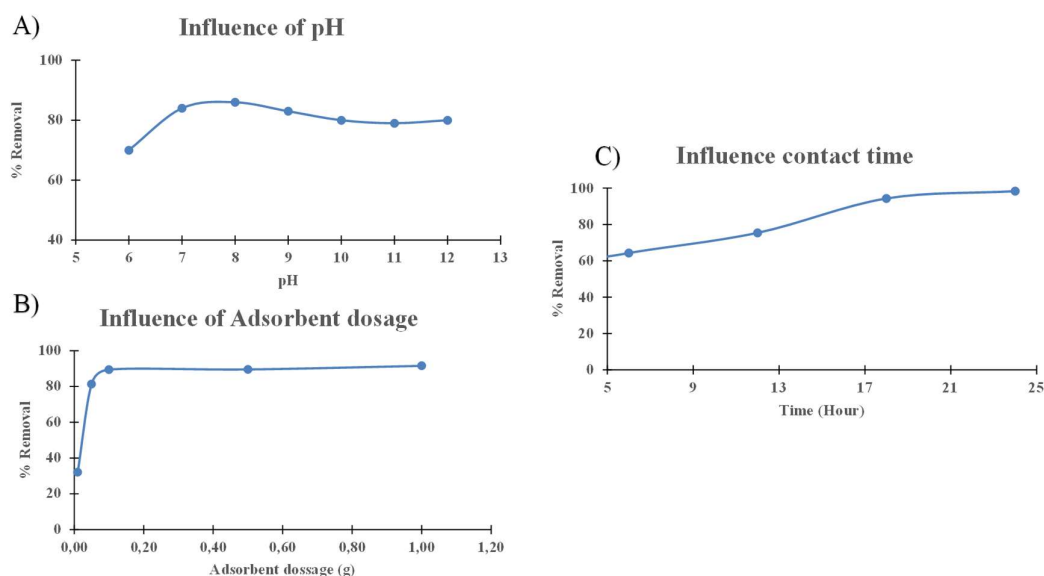

Figure 3. The ACG adsorption of cyanide with pH (A), the adsorbent dosage (B) and the contact time (C) as influencing variables.
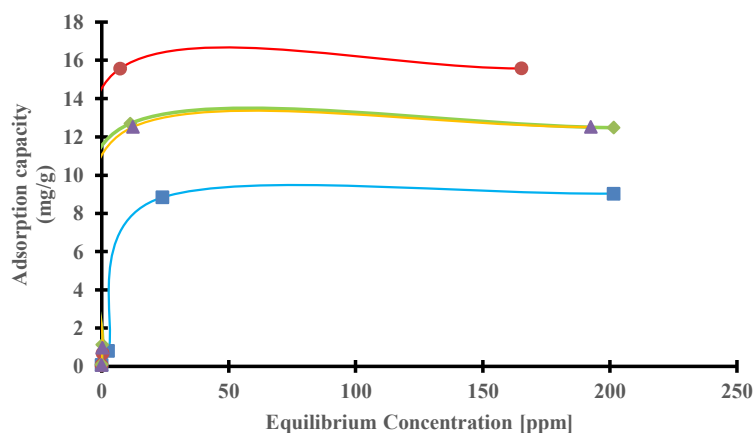

Figure 4. Isotherms for cyanide adsorption on the ACC (red line), the ACA (green line), the ACG (yellow line) and the biomass (blue line).

Table 2. Isotherm adsorption model constant of cyanide.

Adsorbents	Langmuir constant			Freundlich constant		
	q_{max}	b	R^2	K_f	n	R^2
Biomass	0.595	16.5551	0.9857	1.0708	2.03	0.8102
ACC	9.276	1.3560	0.9998	0.6700	1.60	0.9193
ACG	6.993	1.8078	0.9998	0.7098	1.69	0.9076
ACA	3.687	4.3392	0.9981	0.7465	2.03	0.7257

Cyanidation is widely used in industrial gold extraction. Presidential Decree #21 of 2019 regarding the national action plan for mercury elimination demands that all processing that uses liquid mercury must be gradually replaced, especially those employed in ASGM gold extraction. The gold industry uses wastewater plants that control the cyanide pollutants, but in ASGM, the leaching of cyanide will be released into the environment. Cyanide is a harmful and poisonous pollutant whose presence in wastewater and tailings can adversely affect human and environmental health; thus, it is vital to reduce these contaminants in the following years (or decades) (Stavropoulos et al., 2013).

Conclusion

The activated carbon produced from the AGC carbonization process maintains the hydroxyl and carboxyl functional groups on its surface. Besides that, this method can be effectively used at a temperature of 750 °C, since it reduces the amount of ash formed and increases the yield of the activated carbon produced. The highest recorded removal rate of cyanide from wastewater was 98.43%, with an equilibrium reached at a fixed adsorbent dosage of 0.05 g over a contact time of 24 hours. Cyanide adsorption was also shown to be pH-dependent, with the highest cyanide adsorption occurring at a pH of 8. The maximum adsorption capacity for cyanide was 12.51 mg g^{-1} of the adsorbent. The adsorption capacity was also shown to follow a Langmuir isotherm model. These results suggest that a simple method for the preparation of activated carbon can be an effective alternative solution to the problems of traditional miners and can be used with confidence for the removal of cyanide from tailing and leaching wastewater.

Acknowledgements

References

Al-Ghouti, M.A. and Al-Absi, R.S. 2020. Mechanistic understanding of the adsorption and thermodynamic aspects of cationic methylene blue dye onto cellulosic olive stones biomass from wastewater. *Scientific Reports* 10:15928, doi:10.1038/s41598-02 0-72996-3.

Anggraini, D., Soemarno, and Riniwati, H. 2019. The effect of traditional gold mining toward the socio-economic and environmental aspects in Sepauk District Sintang Regency. *Indonesian Journal of Environment and Sustainable Development* 10:51-57, doi:10.21776/ub.jpal.2019.010.01.09.

Ashtaputrey, S.D. and Ashtaputrey, P.D. 2016. Preparation and characterization of activated charcoal derived from orange peel. *Journal of Advanced Chemical Sciences* 2(3):360-362.

ASTM D2866 Standard Test Method for Total Ash Content of Activated Carbon. 2011. ASTM International, West Conshohocken, PA, doi:10.1520/D2866-11.

ASTM D2867 Standard Test Methods for Moisture in Activated Carbon. 2009. ASTM International, West Conshohocken, PA, doi:10.1520/D2867-09.

ASTM D3838 Standard Test Method for pH of Activated Carbon. 2011. ASTM International, West Conshohocken, PA. doi:10.1520/D3838-05R11.

Bansal, R.C. and Goyal, M. 2005. Activation Carbon Adsorption, CRC Press, Boca Raton, doi:10.1201/9781420028812.

Basir-Cyio, M., Isrun-Baso, M., Nakazawa, K., Mahfudz-Muchtar, T., Napitupulu, M., Anshary, A., Rauf, R.A. and Laude, S. 2020. The effect of traditional gold mining to land degradation, mercury contamination and decreasing of agricultural productivity. *Bulgarian Journal of Agricultural Science* 26:612-621.

Bernal, V., Erto, A., Giraldo, L. and Moreno-Piraján, J.C. 2017. Effect of solution pH on the adsorption of paracetamol on chemically modified activated carbons. *Molecules* 22:1-14, doi:10.3390/molecules22071032.

Bhandari, P.S. and Gogate, P.R. 2017. Kinetic and thermodynamic study of adsorptive removal of sodium dodecyl benzene sulfonate using adsorbent based on thermo-chemical activation of coconut shell, *Journal of Molecular Liquids* 252:495-505, doi:10.1016/j.molliq.2017.12.018.

Danish, M., Hashim, R., Ibrahim, M.M.N., Rafatullah, M., Ahmad, T. and Sulaiman, O. 2011. Characterization of *Acacia mangium* wood based activated carbons prepared in the presence of basic activating agents. *Bioresources* 6(3):3019-3033.

De Gisi, S., Lofrano, G., Grassi, M. and Notarnicola, M. 2016. Characteristics and adsorption capacities of low-cost sorbents for wastewater treatment: A review. *Sustainable Materials and Technologies* 9:10-40, doi:10.1016/j.susmat.2016.06.002.

Eke-emezie, N.C. and Etuk, B.R. 2019. Cyanide adsorption from cassava wastewater onto calcined periwinkle shell. *Journal of Degraded and Mining Lands Management* 7(1):1929-1934, doi:10.15243/jdmlm.2019.071.1929.

Efeovbokhan, V.E., Alagbe, E.E., Odika, B., Babalola, R., Oladimeji, T.E., Abatan, O.G. and Yusuf, E.O. 2019. Preparation and characterization of activated carbon from plantain peel and coconut shell using biological activators. *Journal of Physics: Conference Science* 1378:032035, doi:10.1088/1742-6596/1378/3/032035.

Eletta, A., Ajayi, A., Ogunleye, O. and Akpan, C. 2016. Adsorption of cyanide from aqueous solution using calcinated eggshells: Equilibrium and optimization studies. *Journal of Environmental Chemical Engineering* 4:1367-1375, doi:10.1016/j.jece.2016.01.020.

Esparza, M., Cueva, C., Pauker, S., Jentzsch, V. and Bisesti, M. 2019. Combined treatment using ozone for cyanide from wastewater: a comparison. *Revista Internacional de Contaminacion Ambiental* 35:459-467, doi:10.20937/RICA.2019.35.02.16.

Evbuomwan, B.O., Agbede, A.M. and Atuka, M.M. 2013. A comparative study of the physicochemical properties of activated carbon from oil palm waste (kernel shell and fibre). *International Journal of Science and Engineering Investigations* 2:75-79.

Fahmi, A.G., Abidin, Z., Kusmana, C. and Noor, E. 2021 Utilization of palm kernel meal (PKM) as activated

charcoal to remove organic pollutants. *Journal of Physics: Conference Science* 1882:012117, doi:10.1088/1755-1315/399/1/012015.

Fahmi, A.G., Abidin, Z., Kusuma, C., Kharisma, D., Prajaputra, V. and Rahmawati, W.R. 2019. Preparation and characterization of activated carbon from palm kernel shell at low temperature as an adsorbent for methylene blue. *IOP Conference Series: Earth and Environmental Science* 399:012015, doi:10.1088/1742-6596/1882/1/012117.

Gafur, N.A., Sakakibara, M., Komatsu, S., Sano, S. and Sera, K. 2022. Environmental survey of the distribution and metal contents of *Pteris vittata* in arsenic-lead-mercury-contaminated gold mining areas along the Bone River in Gorontalo Province, Indonesia. *International Journal of Environmental Research and Public Health* 19:530, doi:10.3390/ijerph19010530.

Githiria, J.M. and Onifade, M. 2020. The impact of mining on sustainable practices and the traditional culture of developing countries. *Journal of Environmental Studies and Sciences* 10:394-410, doi:10.1007/s13412-020-00613-w.

Han, K., Wang, Q., Zhao, J., Luo, K.H., Chen, Y. and Lu, C. 2016. Combustion pattern, characteristics, and kinetics of biomass and chars from segmented heating carbonization. *Asia-Pacific Journal of Chemical Engineering* 11:812-822, doi:10.1002/apj.2016.

Hou, D., Liu, L., Yang, Q., Zhang, B., Qiu, H., Ruan, S., Chen, Y. and Li, H. 2020. Decomposition of cyanide from gold leaching tailings by using sodium metabisulphite and hydrogen peroxide. *Advances in Materials Science and Engineering* 2020:1-7, doi:10.1155/2020/5640963.

Istratie, R., Stoia, M., Păcurariu, C. and Locovei, C. 2019. Single and simultaneous adsorption of methyl orange and phenol onto magnetic iron oxide/carbon nanocomposites. *Arabian Journal of Chemistry* 12:3704-3722, doi:10.1016/j.arabjc.2015.12.012.

Jaszczak, E.. Polkowska, Z.: Narkowicz, S. and Namieśnik, J. 2017. Cyanides in the environment-analysis-problems and challenges. *Environmental Science and Pollution Research International* 24:15929-15948, doi:10.1007/s11356-017-9081-7.

Jeon, C., Lee, J., Chung, H., Kim, J. and Park J. 2017. A study on insulating characteristics of glass wool and mineral wool coated with a polysiloxane agent. *Advances in Materials Science and Engineering* 3938965:1-6, doi:10.1155/2017/3938965.

Jiao, C.Y., Wan, C. and Li, J. 2016. Synthesis of carbon fiber aerogel from natural bamboo fiber and its application as green high-efficiency and recyclable adsorbent. *Materials and Design* 107:26-32, doi:10.1016/j.matdes.2016.06.015.

Johnson, A. 2015. The fate of cyanide in leach wastes at gold mines: an environmental perspective. *Applied Geochemistry.* 57:194-205, doi:10.1016/j.apgeochem.2014.05.023.

Knoblauch, A.M., Farnham, A., Ouoba, J., Zanetti, J., Müller, S., Jean-Richard, V., Utzinger, J., Wehrli, B., Brugger, F., Diagbouga, S. and Winkler, M.S. 2020. Potential health effects of cyanide use in artisanal and small-scale gold mining in Burkina Faso. *Journal of Cleaner Production* 252:11968, doi:10.1016/j.jclepro.2019.119689.

Kubik, L. and Zeman, S. 2014. Determination of oxygen permeability and mechanical properties of the

aluminium paper foil. *Research in Agricultural Engineering* 60(4):172-179, doi:10.17221/18/2013-RAE.

Li, X., Xiao, W., He, G., Zheng, W., Yu, N. and Tan, M. 2012. Pore size and surface area control of MgO nanostructures using a surfactant-templated hydrothermal process: High adsorption capability to azo dyes. *Colloids and Surfaces. Part A: Physicochemical and Engineering Aspects* 408:79-86, doi:10.1016/j.colsurfa.2012.05.034.

Mariana, M., Mahidin, M., Maulana, F. and Aman, F. 2017. Utilization of Activated Carbon Prepared from Aceh Coffee Grounds as Bio-sorbent for Treatment of Fertilizer Industrial Waste Water. *IOP Conference Series: Materials Science and Engineering* 358:012027, doi:10.1088/1757-899X/358/012027.

Munera-Echeverri, J.L., Martinsen, V., Strand, L.T., Zivanovic, V., Cornelissen, G. and Mulder, J. 2018. Cation exchange capacity of biochar: an urgent method modification. *Science of the Total Environment* 642:190-197, doi:10.1016/j.scitotenv.2018.06.017.

Muslihudin, M., Bambang, A.N., Hendarto, E. and Putranto, T.T. 2018. The impact of traditional gold mining in Gumelar Banyumas, Indonesia. *Ecology, Environment and Conservation* 28:607-613.

Okeola, O.F., Odebunmi, E.O. and Ameen, O.M. 2012. Comparison of sorption capacity and surface area of activated carbon prepared from *Jatropha curcas* fruit pericarp and seed coat. *Bulletin of the Chemical Society of Ethiopia* 26:171-180, doi:10.4314/bcse.v26i2.2.

Park, S. 2018. Physico-chemical and anatomical properties of carbonized Indonesian bamboo and its appropriate utilization, IPB University, Bogor**.**

Park, S.B., Lee, S.M., Vetter, J.Y. and Lee, S.H. 2009. Manufacture of crack-free carbonized board from fiberbroad, *Journal of the Korean Wood Science and Technology* 37:293-299.

Prasetia, H., Sakakibara, M., Sera, K. and Laird, J.S. 2022. Evaluation of the total mercury weight exposure distribution using tree bark analysis in an artisanal and small-scale gold mining area, North Gorontalo Regency, Gorontalo Province, Indonesia. *International Journal of Environmental Research and Public Health* 19:33, doi:10.3390/ijerph19010033.

Sivakumar, V., Asaithambi, M. and Sivakumar, P. 2012. Physico-chemical and adsorption studies of activated carbon from agricultural waste. *Advances in Applied Science Research* 3:219-226.

Soemarwoto, R. and Ellen, R.F. 2010. Gold mining and changing perceptions of risk in West Java. *Human Organization* 69:233-241, doi:10.17730/humo.69.3.gk887801m1476105.

Stavropoulos, G.G., Skodras, G.S. and Papadimitriou, K.G. 2013. Effect of solution chemistry on cyanide adsorption in activated carbon. *Applied Thermal Engineering* 74:183-184, doi:10.1016/j.applthermaleng.2013.09.060.

Suhadi, S., Muliya, B.K. and Ashoffi, A.M. 2021. Pollution of mercury and cyanide soils and plants in surrounding in the artisanal and small-scale gold mining (ASGM) at Sekotong District, West Lombok, West Nusa Tenggara. *Biological Environment and Pollution* 1:30-37, doi:10.31763/bioenvipo.v1i1.392.

Sun, K., Leng, C., Jiang, J., Bu, Q., Lin, G., Lu, X. and Zhu, G. 2017. Microporous activated carbon from coconut shells produced by self-activation using the pyrolysis gases produced from them, that have an excellent electric

double layer performance. *New Carbon Materials* 32:451-459, doi:10.1016/S1872-5805(17)60134-3.

Surleva, A., Zaharia, M., Ion, L., Gradinaru, R.V., Drochioiu, G. and Mangalagiu, I. 2013. Ninhydrin-based spectrophotometric assays of trace cyanide. *Acta Chemica Iasi* 21:57-70, doi:10.2478/achi-2013-0006.

Tabian, D., Bulgaru Iliescu, D., Diac, M.M., Badea, M., Toma, S.I. and Drochioiu, G. 2022. Evaluation of hydrogen cyanide in the blood of fire victims based on the kinetics of the reaction with ninhydrin. *Applied Sciences* 12:2329, doi:10.3390/app12052329.

Taux, K., Kraus, T. and Kaifie, A. 2022. Mercury exposure and its health effects in workers in the artisanal and small-scale gold mining (ASGM) sector-a systematic review. *International Journal of Environmental Research and Public Health* 19:2081, doi:10.3390/ijerph19042081.

US EPA. 2020. Clarification of Free and Total Cyanide Analysis for Safe Drinking Water Act (SDWA) Compliance, Environment Protection Agency: Washington.

Verbrugge, B., Lanzano, C. and Libassi, M. 2021. The cyanide revolution: efficiency gains and exclusion in artisanal and small-scale gold mining. *Geoforum* 126:267-276, doi:10.1016/j.geoforum.2021.07.030.

Xiao, F., Bedane, A.H., Zhao, J.X., Mann, M.D. and Pignatello, J.J. 2018. Thermal air oxidation changes surface and adsorptive properties of black carbon (char/biochar). *Science of the Total Environment* 618:276-283, doi:10.1016/j.scitotenv.2017.11.008.

Yakout, S.M. and El-Deen, G.S. 2016. Characterization of activated carbon prepared by phosphoric acid activation of olive stones. *Arabian Journal of Chemistry* 9:S1155-S1162, doi:10.1016/j.arabjc.2011.12.002.